Effect of microwave-induced chemical modification of kaolinite and its application as an eco-friendly filler of rubber blends

Andrea Feriancová[1),*)] (ORCID ID: 0000-0003-2293-5213), **Jana Šulcová**[1)] (0000-0002-1148-2581), **Jana Pagáčová**[1)] (0000-0003-3639-6492), **Andrej Dubec**[1)] (0009-0001-6145-6357), **Iveta Papučová**[1)] (0000-0002-3626-4783), **Mariana Pajtášová**[1)] (0000-0001-7834-977X), **Darina Ondrušová**[1)] (0000-0003-2167-9174), **Silvia Ďurišová**[1)] (0000-0002-2268-7742), **Maroš Dedinský**[1)] (0000-0003-2315-3926), **Tomasz Waldemar Klepka**[2)] (0000-0001-9182-0845)

DOI: https://doi.org/10.14314/polimery.2025.3.2

Abstract: Kaolinite was subjected to microwave (MW) and chemical modification with silane and copper acetate. The process was carried out for 30, 60 and 120 min. The use of microwave radiation shortened the time of kaolinite modification (from several days to 30 min). The presence of modifying compounds in the kaolinite structure was confirmed by FT-IR, DSC, TGA and SEM. The use of modified kaolinite (10 phr) reduced the rate of vulcanization of natural rubber and facilitated its processing. Moreover, silane-modified kaolinite increased the tensile strength and hardness of natural rubber, which indicates its strengthening effect.

Keywords: modified kaolinite, rubber composites, microwave radiation, thermal analysis, FT-IR.

Wpływ mikrofal na modyfikację chemiczną kaolinitu i jego zastosowanie jako ekologicznego napełniacza mieszanek gumowych

Streszczenie: Kaolinit poddano działaniu mikrofal (MW) oraz modyfikacji chemicznej silanem i octanem miedzi. Proces prowadzono przez 30, 60 i 120 min. Zastosowanie promieniowania mikrofalowego skróciło czas modyfikacji kaolinitu (z kilku dni do 30 min). Obecność związków modyfikujących w strukturze kaolinitu potwierdzono metodą FT-IR, DSC, TGA i SEM. Zastosowanie modyfikowanego kaolinitu (10 phr) zmniejszyło szybkość wulkanizacji naturalnego kauczuku i ułatwiło jego przetwórstwo. Ponadto kaolinit modyfikowany silanem zwiększył wytrzymałość na rozciąganie i twardość kauczuku naturalnego co świadczy o jego wzmacniającym działaniu.

Słowa kluczowe: modyfikowany kaolinit, kompozyty gumowe, promieniowanie mikrofalowe, analiza termiczna, FT-IR.

Clay mineral/rubber composites are a subject of research interest due to their significantly improved properties in comparison with the primary polymers. In general, rubber composites are mostly filled with carbon black fillers which have some disadvantages, for example high heat generation at higher loading, health risks for operators, and the risk of environmental pollution. Therefore, it is being replaced by silica, aluminosilicates, calcium carbonate, or oxides. Kaolin is used in rubber compounds due to its environmental character, low price, good plasticity, dispersibility, better heat resistance, and assignability as a partially reinforcing filler. Kaolinite is clay mineral belonging to the phyllosilicate group [1, 2]. Crystal structure of kaolinite, composed of 1:1 type of a two-layer structure, affects significant properties such as low surface charge, low surface area, inert character in a wide range of pH, as well as pseudohexagonal lamellar particle shape [3, 4]. The kaolinite consists of two types of layers: the octahedral sheet (with central Al^{III} atoms), covered by hydroxy groups (–OH) and the tetrahedral sheet (with central Si^{IV} atoms) with the least reactive siloxane groups (Si–O) [5]. Properties such as: specific surface area, good dispersion, and good filler-elastomer inter-

[1)] Department of Materials Technologies and Environment, Faculty of Industrial Technologies in Púchov, Alexander Dubček University of Trenčín, I. Krasku 491/30, 020 01 Púchov, Slovak Republic.

[2)] Department of Technology and Polymer Processing, Faculty of Mechanical Engineering, Lublin University of Technology, ul. Nadbystrzycka 36, 20-618 Lublin, Poland.

[*)] Author for correspondence: andrea.feriancova@tnuni.sk

action are important for the application of kaolinite in technical rubber [6-8].

Various modification techniques are used to change the properties of kaolinite and to improve dispersion of its particles in polymer matrix. Currently, the preparation of organo-kaolinites focusses on the properties of the organic substances used or on the conditions of reaction [9]. Different reagents with small molecules such as potassium acetate [10, 11], dimethyl sulfoxide [12], urea [13, 14], and hydrazine [15] are used. Quaternary ammonium salts [16], fatty acid salts [17], or silanes [18] were used as macromolecular intercalants.

By calcination [19], exfoliation by ultrasonic wave treatment [20], or by microwave treatment [21, 22], the improvements in desired properties of kaolinite can be achieved. Heating using microwave (MW) radiation enables the reaction temperature to be quickly reached in the entire volume of the sample, while the substances or solvents themselves can also take part in the heating [23]. By water molecules, the effect of electromagnetic field of microwave radiation on layered silicates is absorbed.

In this study, the intercalation of natural kaolinite with copper acetate and (3-aminopropyl)-triethoxysilane (APS) solution was investigated. Silanes and transition metals (such as Cu^{2+}) are important precursors that can affect good adhesion between rubber components [24]. The kaolinite intercalation reactions were carried out in a laboratory-scale microwave reactor with a built-in IR temperature sensor and stirrer. In the amount of 10 phr and in combination with carbon black (CB), the modified kaolinite was used in SMR/kaolinite composites. The effect of chemical/MW treatment of kaolinite on the curing, physical and mechanical properties of SMR/kaolinite composites was evaluated.

EXPERIMENTAL PART

Materials and chemical/MW treatment of kaolinite

According to [25], chemical/MW treatment of kaolinite (Ka) was carried out. In this study, Ka from LB Minerals Kaznějov (Czech Republic) with a particle size of 45 μm was used. The composition of the main oxides was as follows: SiO_2 60.8 wt%, Al_2O_3 34.7 wt%, K_2O 1.6 wt%, SO_3 0.6 wt%, and the loss on ignition of Ka at 1000°C was 8.62 wt%. Copper acetate ($Cu(CH_3COO)_2$ H_2O), sodium hydroxide (NaOH) and ethanol were purchased from Merck (Rahway, NJ, USA), (3-aminopropyl)triethoxysilane (APS) was purchased from Aldrich Chemical Company Inc. (Burlington, MA, USA). All chemicals used were of analytical grade.

Mechanical conditioning of kaolinite was performed using a cutting mill SM300 (Retsch GmbH, Haan, Germany) at 2000 rpm with 6-disc rotor with a 0.25 mm mesh trapezoidal screen.

Chemical conditioning of kaolinite was achieved as follows: sample was treated with 0.3 M solution of copper acetate (CuA) for 15 min, then the 0.3 M NaOH solution was added. Within the silane treatment kaolinite was dispersed in solution of APS, ethanol, and distilled water (in a ratio of 3:90:10). All dispersions were modified under the vigorous stirring in microwave reactor FlexiWAVE (Milestone Srl, Sorisole, Italy) with solid-phase configuration at a constant temperature of 80°C and at time intervals of 30, 60, and 120 min. Intercalates were washed three times with distilled water and/or ethanol and then they were centrifuged for 10 min at 2000 rpm. Samples treated with CuA were designated: K-Cu1 (30 min), K-Cu2 (60 min), K-Cu3 (120 min), the silanized samples were designated: K-A1 (30 min), K-A2 (60 min), and K-A3 (120 min). All chemically/MW treated samples were dried in an oven at 60°C for 8 h.

Kaolinite characterization

To assess the chemical composition of Ka, the energy dispersive X-ray spectroscopy analysis EDX (Shimadzu EDX-7000, Kyoto, Japan) was utilized. The FT-IR Nicolet iS50 Thermo Scientific spectrometer (Waltham, MA, USA) in the range 4000–400 cm^{-1} with ATR mode was used (resolution of 4 cm^{-1} and 32 scans, diamond crystal). Scanning electron microscopy images were taken, using VEGA 3 TESCAN microscope (Brno, Czech Republic), with BSE detector and field of view 40 mm with Wide Field Optics, magnified 4000–12000×. The TG/DSC measurements, using TGA/DSC 2 STAR^e System Mettler Toledo (Greifensee, Switzerland), were carried out in N_2 atmosphere, heating rate of 5°C/min^1 up to 700°C, the sample mass was 20–24 mg.

SMR/kaolinite composites preparation and characterization

To prepare a composite, natural rubber (SMR 10, Resinex, Czech Republic) was used as a matrix. The formulation of components used is listed in Table 1. To form a composite, a two-step blending process was used, following materials added:

Step 1: 100 phr (parts per hundred rubber) of SMR 10 (Resinex, Czech Republic) with a density of 0.91 g/cm^3; 5.0 phr of activators: zinc oxide (SlovZinc, a.s., Košeca, Slovakia) with a density of 5.68 g/cm^3 and stearic acid (Aldrich Chemical Company Inc., Burlington, MA, USA) with a density of 0, 94 g/cm^3; 39.0 phr of Carbon black N339 (CB) (MAKROchem, Lublin, Poland); 10.0 phr of MW/modified kaolinite: K-Cu1, K-Cu3, K-A1, and K-A3; 3.5 phr of antidegradants 6PPD (with a density of 1.06 g/cm^3), DTPD (antioxidant of high grade), TMQ (Dusantox, Duslo a.s., Šaľa, Slovakia);

Step 2: 1.7 phr of curing agent – sulfur (Istrochem a.s., Bratislava, Slovakia), and 1.0 phr of a slow accelerator CBS (Istrochem a.s., Bratislava, Slovakia). The SMR/kaolinite composites were prepared in Plasti-Corder Brabender®EC plus (Duisburg, Germany) at a temperature of 90°C in

T a b l e 1. Composition of Ka/SMR composites

Ingredients, phr*)	ST/CB	Ka/SMR	K-Cu1/SMR K-Cu3/NR	K-A1/SMR K-A3/SMR
SMR 10	100.0	100.0	100.0	100.0
ZnO	3.0	3.0	3.0	3.0
Stearic acid	2.0	2.0	2.0	2.0
Antidegradants	3.5	3.5	3.5	3.5
CB	49.0	39.0	39.0	39.0
Kaolinite	–	10.0	10.0	10.0
CBS	1.0	1.0	1.0	1.0
Sulfur	1.7	1.7	1.7	1.7

phr*) – parts per hundred

step 1 (time 7 min) and at a temperature of 90°C in step 2 (mixing time 5.5 min), with constant speed of 50 rpm. Using a hydraulic press LabEcon 600 Fontijne (Rotterdam, The Netherlands), the individual SMR/kaolinite composites were cured (vulcanized) under the pressure of 20 MPa at 160°C.

The curing characteristics and torque of SMR/kaolinite composites were evaluated using an oscillating rheometer RPA-2000 (Alpha Technologies, Akron, OH, USA) at 160°C for 20 min. The curing rate index (CRI) was calculated as follows: CRI = $[100/(t_{90}–ts_2)]$, where t_{90} is the optimum curing time and ts_2 is the scorch time. The storage shear moduli G′ (Payne effect determination) were evaluated using an RPA 2000 rheometer at 70°C, 170°C (curing) and after cooling to 70°C, at a frequency of 1 Hz and strains ranging from 0.28% to 100.02%. The Payne effect was assessed by the difference in shear moduli at low (0.28%) and high strain (100.02%).Using scanning electron microscope VEGA 3 TESCAN, magnified 500–6000×, the dispersion of kaolinite filler in the SMR/kaolinite composites was studied. Via universal tensile machine Autograph AG-X plus 5kN, Shimadzu (Kyoto, Japan), the tensile properties (tensile strength Ts_b and elongation at break E_b) were measured. As given in ASTM D-412, the speed of testing machine was 500 mm/min[1]. According to the ASTM D2240, and by using Durometer Shore A, the hardness was determined.

RESULTS AND DISCUSSION

Kaolinite characterization

In Fig. 1, FT-IR spectra of Ka and modified kaolinite (K-Cu1, K-Cu2, K-Cu3) after MW radiation (30, 60, and 120 min, respectively) are shown. In the natural Ka (Fig. 1 red curve), the bands corresponding to the stretching vibration of inner-surface –OH (ν(*ou*OH)) groups at 3685, 3668, and 3650 cm^{-1} were observed. The band at 3618 cm^{-1} is related to the stretching vibration of the inner –OH ν(inOH) group between the tetrahedral and octahedral sheet. At a wavenumber of 910 cm^{-1} the bending vibration of Al–OH group (in the region of 1650–650 cm^{-1}) is seen [26, 11, 27]. At 1024 and 998 cm^{-1}, the stretching vibrations of the Si–O bonds were observed. The doublet at 795–750 cm^{-1} is characteristic of the valence and deformation modes of the Si–O–Al bond [9, 28, 29]. In the IR spectra of modified K-CuX samples (blue and violet curve), the decrease in relative intensity and a slight shift to a higher value of the external hydroxyl group ν(ouOH) were observed. The IR spectra of modified K-CuX sam-

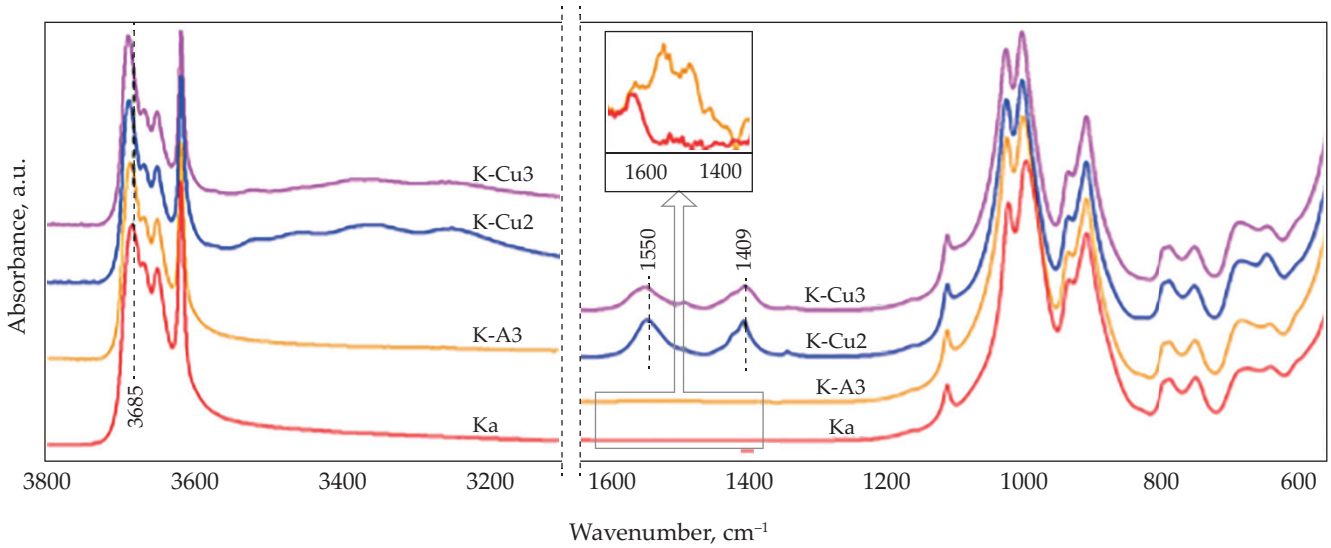

Fig. 1 FT-IR spectra of Ka, K-Cu2, K-Cu3 and K-A3 in selected regions

T a b l e 2. Chemical composition of natural and modified kaolinite

Sample, wt%	Ka	K-Cu1	K-Cu2	K-Cu3	K-A1	K-A2	K-A3
SiO_2	60.8	53.3	52.1	53.8	60.9	60.9	61.2
Al_2O_3	34.7	30.3	30.4	31.3	34.9	34.8	34.5
CuO	–	12.2	13.1	10.9	–	–	–
K_2O	1.6	1.6	1.6	1.6	1.8	1.7	1.7
SO_3	0.6	1.0	1.1	0.7	0.8	0.8	0.9

ples in the 1650–650 cm^{-1} region show the presence of absorption bands at 1550 and 1409 cm^{-1} that are related to the asymmetric and symmetric stretching vibrations of the carboxylate group ν_a(COO–) and ν_s(COO–) [30]. From the conclusions of previous research [6, 10, 31] it is possible to confirm the formation of a monohydrate copper hydroxy acetate complex. This assumption is supported by small new shoulders in the region 3450–3249 cm^{-1}, which are attributed to molecules of water coordinated through this new complex. A weaker band observed at 648 cm^{-1} (K-Cu2) can be assigned to the Cu–OH deformation [32].

After silanization, a small displacement of the characteristic kaolinite bands to higher wavenumbers in the spectra of K-A3 was observed, and the intensity of stretching vibration ν(*ou*OH) at 3685 cm^{-1} increased. All silanized samples exhibited weak bands at 2932 cm^{-1}, 1490 cm^{-1}, and 683 cm^{-1}, which were assigned to the vibration of $–CH_2$ group [33, 34]. A small band at 1559 cm^{-1} can be ascribed to the vibration of the N–H group.

In Table 2 the chemical composition of Ka and kaolinite after chemical/MW treatment for 30, 60, and 120 min is listed. The sample of Ka has a high SiO_2 content (60.8 wt%) followed by 34.7 wt% of Al_2O_3 and the small amount of K_2O (1.6 wt%). After chemical/MW treatment of Ka with copper acetate, the presence of copper, expressed as CuO. At a treatment time of 60 min., the highest amount of CuO in K-Cu2 (13.1 wt%) was observed, while the lowest amount of copper was recorded for K-Cu3 (at a treatment time of 120 min). This result can be explained by the fact that longer exposure to MW radiation led to partial degradation of the bounded copper compound. After silanization, the higher content of silica (61.2 wt%), at a modification time of 120 min. (K-A3), was recorded.

Obtained samples of the modified kaolinite samples were examined using TGA and DSC, analysis (Fig. 2), the thermal properties of were recorded. The endothermic effect on the curve Ka in Fig. 2a, with the maximum at 510°C, is attributed to the dehydroxylation of kaolinite, which involves the removal of structural water [27, 35]. Mass loss of natural Ka, recorded at 700°C, was 8.5 wt% (Fig. 2b, Table 3). All modified K-CuX samples demonstrated one significant mass loss to temperature of 350°C. For the K-Cu2 sample (Fig. 2a), the observed mass loss within the temperature range of 120–350°C (6.3 wt%) can be ascribed to the volatilization of the intercalated copper hydroxy acetate complex [32]. A pronounced exothermic effect at 274°C (Fig. 2b, blue curve) is attributed to the decomposition of organic copper salts. The mass loss observed in the K-Cu2 and K-Cu3 samples within the temperature range of 350–700°C (Fig. 2a), with an endothermic maximum at 520°C (Fig. 2b), indicates that the copper acetate treatment increased the dehydroxylation temperature of kaolinite by 11–13°C. This may be attributed to the adhesion effect occurring within the kaolinite sheets influenced by the presence of Cu^{2+} ions [6]. The total mass loss for the K-Cu1, K-Cu2, and K-Cu3 samples was 12.8, 13.2, and 11.9 wt%, respectively (Table 3), which is consistent with the results obtained from elemental analysis.

The TG/DSC curves of silanized K-AX samples exhibited a consistent pattern. The mechanism illustrating the mass

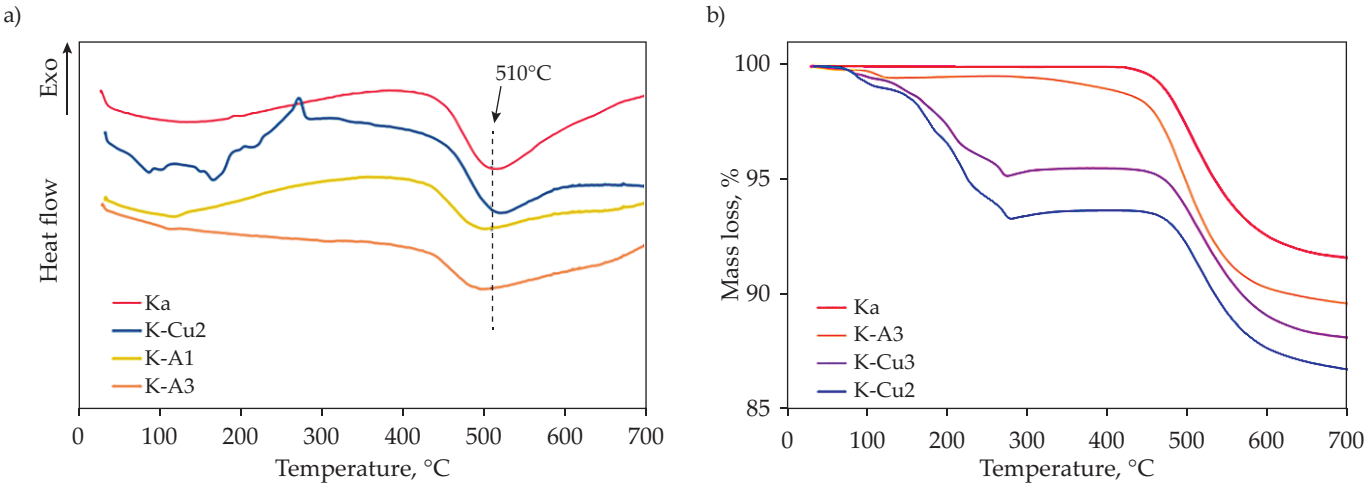

Fig. 2. Thermal analysis of natural and selected modified kaolinite: a) DSC, b) TGA

losses of K-A3 is represented by the yellow curve in Fig. 2a. The initial minor mass loss (0.9 wt%) observed within the temperature range of ~ 119–350°C is due to the volatilization of hydrogen-bonded APS [22]. The subsequent mass loss of 9.5 wt% (Table 3), occurred within the temperature range of 350–700°C with an endothermic peak (Fig. 2b) centered at 496°C, attributed to the dehydroxylation of kaolinite, which is shifted to lower temperature compared to Ka. This occurrence may result from the intercalation of organo-silane groups grafted onto the kaolinite.

To detect micromorphological changes for modified kaolinite samples, scanning electron microscope was used. SEM image (Fig. 3a) shows aggregates of natural Ka composed of tabular particles which are usually of regular hexagonal shape [36]. The layered structure of kaolinite is certainly visible. Between the layers (lamellas) there is an empty microspace, which is created by an imper-

T a b l e 3. Thermal analysis

Sample	Weight loss in interval 30–350°C, wt%	Weight loss in interval 350–700°C, wt%	Dehydroxylation temperature, °C
Ka	0.2	8.5	510
K-Cu1	5.6	7.2	520
K-Cu2	6.3	6.9	520
K-Cu3	4.5	7.4	522
K-A1	0.9	9.4	502
K-A2	0.6	9.7	501
K-A3	0.9	9.5	496

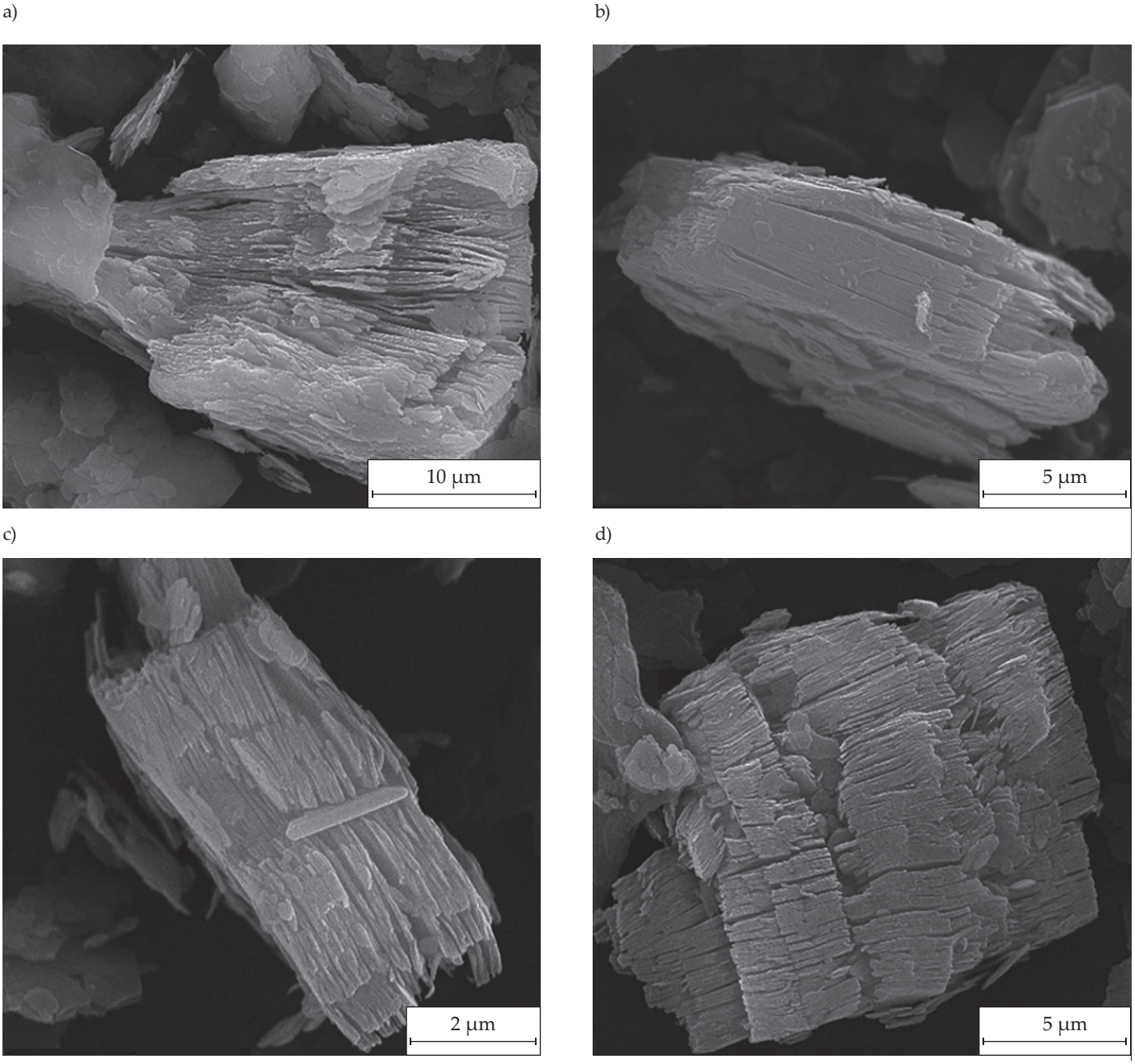

Fig. 3. SEM micrographs: a) Ka, b) K-Cu2, c) K-A2, d) K-A3

fect connection of the surfaces of the individual layers. In the K-Cu2 sample in Fig. 3b, the kaolinite particle is formed by well-fitting layers with a small free microspace, which locally reaches the larger geometric dimensions. Defragmentation of the kaolinite layers is mostly not observed. Compared to Ka, the surface of this modified sample looks more compact and may be caused by the higher adhesion between the kaolinite sheets in which the Cu^{2+} ions are present. This observation confirmed the assumptions from the results of the thermal analysis.

When the silanizing agent APS was used, the most significant changes in the structure of the samples were observed. The kaolinite particle of sample K-A2 (Fig. 3c) is formed by sheets which are noncompact, in the form of several separate segments. On the surface, it is possible to observe a stepped relief with a larger amount of free microspace between the individual sheets. For the K-A3 sample (Fig. 3(d)), the changes are more pronounced than for the K-A2 sample. A distinct stepped microrelief of K-A3 is visible in the kaolinite particle. A large amount of free space is present between the layers, on which a considerable degree of defragmentation is observed. We observe significant enlargement of the kaolinite unit (particles) in the K-A3 sample and the enlargement or swelling of the individual lamellae, which show a more ordered structure compared to other samples of modified as well as raw kaolinite and could be caused by a longer reaction time to MW heating.

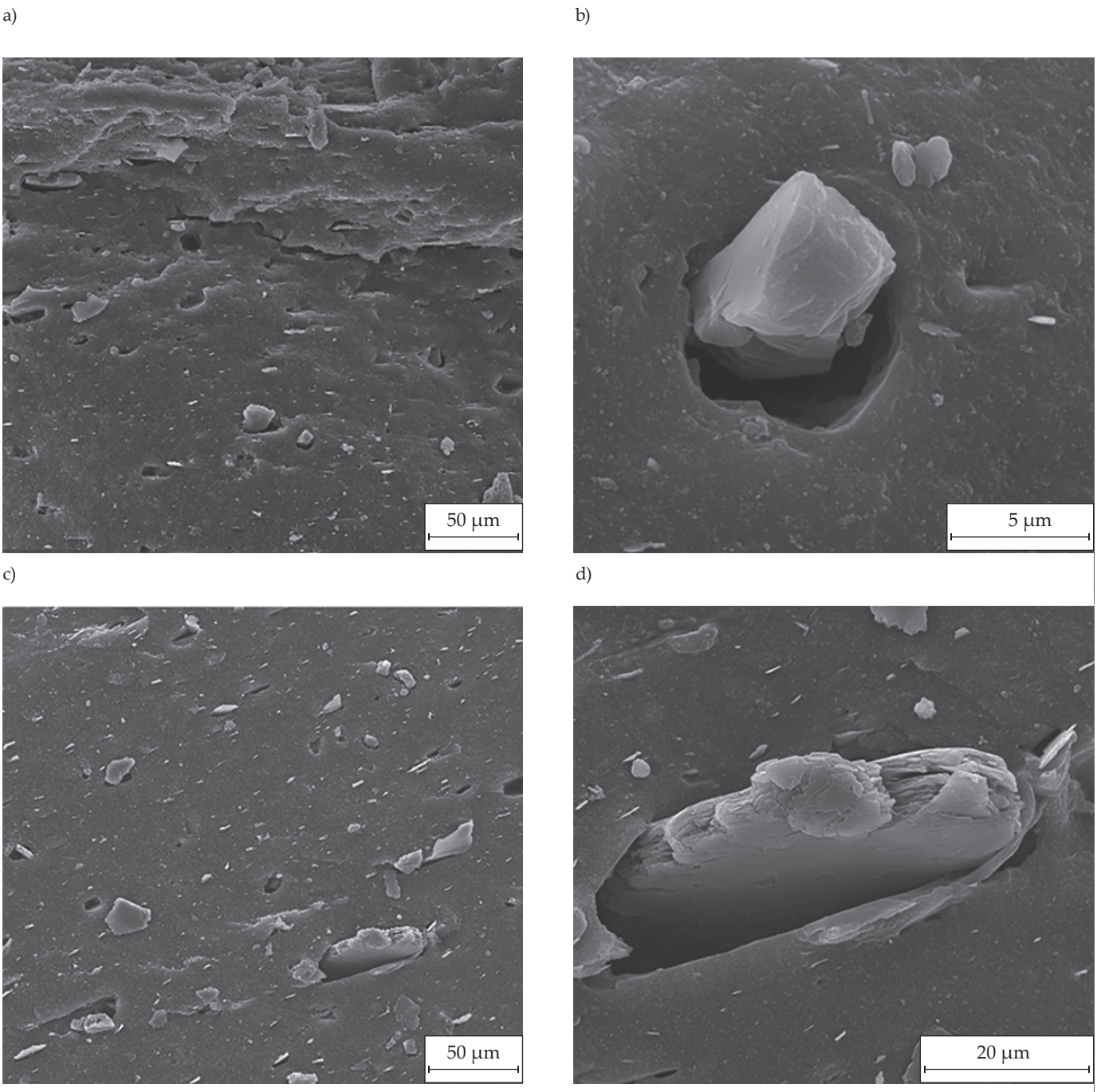

Fig. 4 SEM micrographs of kaolinite/SMR composites: a) K-Cu2/SMR, b) K-Cu2/SMR detail, c) K-A3/SMR, d) K-A3/SMR

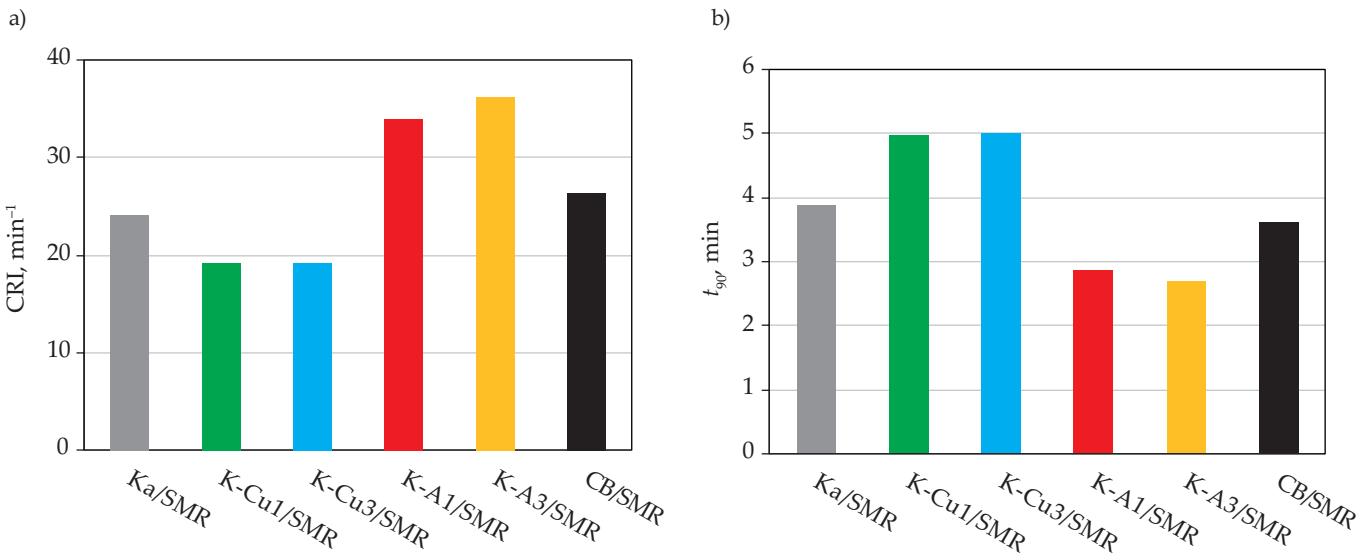

Fig. 5 Processing characteristics of kaolinite/SMR composites: a) CRI coefficient, b) cure time t_{90}

SEM analysis of kaolinite/SMR composites

Fig. 4 presents SEM micrographs illustrating the tensile fracture surfaces of K-Cu3/SMR and K-A3/SMR composites, respectively. The dispersion of the K-Cu3 particles appears to be uniform, with no significant agglomerates present in the elastomeric matrix (Fig. 4a). A detailed examination of the kaolinite particle integrated within the elastomeric matrix in Fig. 4b reveals the existence of a free microspace between the particle's surface and the rubber matrix. Notably, no free fragments of the kaolinite layers are observed.

This observation could affirm the superior coherence of the kaolinite particle. Additionally, the absence of a free microspace on the particle's surface is noted. Within the micro area surrounding the particle, no further imperfections within the elastomeric matrix are detectable. It is improbable that the kaolinite particle induces a substantial notching effect.

The dispersion of the kaolinite particles in K-A3/SMR is uniform (Fig. 4c). No agglomerates were observed after incorporation of the filler into the elastomeric matrix. In Fig. 4d the empty microspace is visible around the K-A3 particle. It is possible to see the decohesion's on the kaolinite layers, as well as the individual fragments of the layers. The free microspace between the layers of the kaolinite particles is observed. No other imperfections of the elastomeric matrix are visible in the micro area where the particle is located.

Curing and processing characteristics of kaolinite/SMR composites

Good processability as well as safe and fast curing (vulcanization) are fundamental parameters in the creation of rubber products. Table 4 presents the curing characteristics of kaolinite/SMR composites containing 10 phr loading of natural Ka or modified kaolinite samples (K-Cu1, K-Cu3, K-A1, K-A3) and their comparison with the standard utilizing CB. It is evident that for composites Ka/SMR, K-Cu1/SMR, and K-Cu3/SMR, the curing reaction is delayed. The composites exhibited the lowest curing rate index CRI (min^{-1}) (Fig. 5a) and a correspondingly increased cure time t_{90} (Fig. 5b).

Copper cations Cu^{2+} possess a high affinity for sulfur, forming sparingly soluble compounds, and thus can function as vulcanization inhibitors, consequently reducing the curing rate [10, 37]. The extension of the cure time may have specific application purposes, particularly in applications requiring thick-walled products. Conversely, the silanized samples K-A1 and K-A3 exhibited an enhancement in the reduction of cure time and an acceleration of the curing rate. The silane modified kaolinite surface may participate in the formation process

T a b l e 4. Curing and processing parameters of kaolinite/SMR composites

Composite	t_{s2} min	t_{90} min	M_L dNm	M_H dNm	CRI min^{-1}
Ka/SMR	1.66	3.89	3.13	28.29	24.05
K-Cu1/SMR	0.90	4.96	3.16	27.50	19.26
K-Cu3/SMR	0.88	5.00	3.19	27.97	19.12
K-A1/SMR	0.98	2.87	3.50	29.56	33.86
K-A3/SMR	0.92	2.70	3.82	29.92	36.12
CB/SMR	1.28	3.61	3.56	31.39	26.42

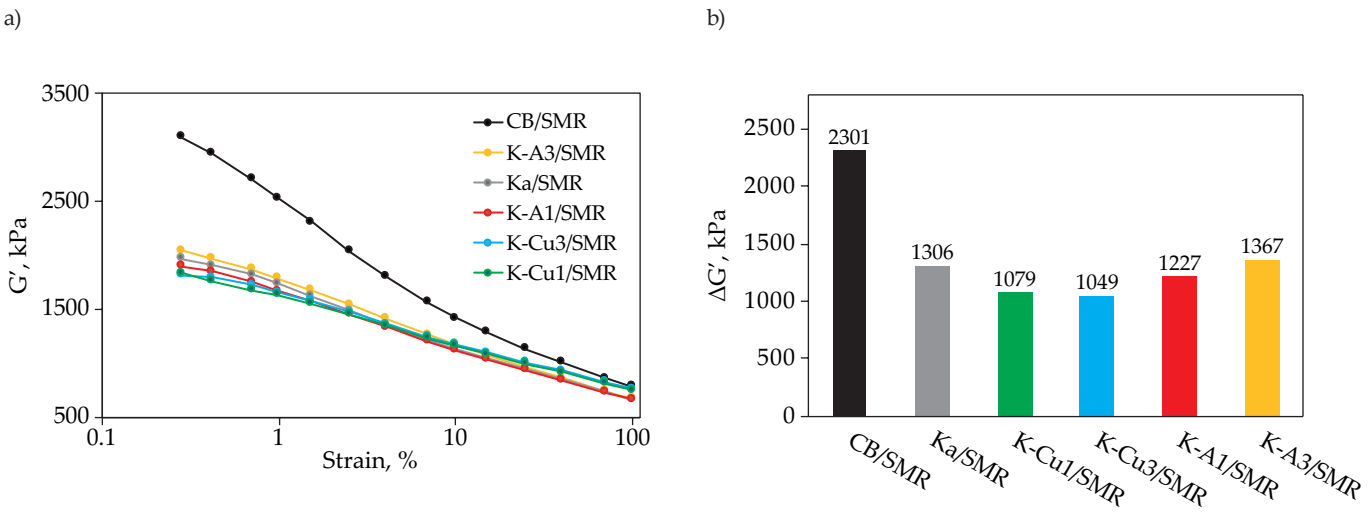

Fig. 6. Charts presenting: a) strain amplitude vs. shear modulus *G′*, b) Payne effect Δ*G′* of SMR/kaolinite composites

of an active sulfur curing agent, thus contributing to the expedited crosslinking of the rubber network [18]. In the context of blending, extrusion, molding, and filling into molds, increasing the scorch time is advantageous.

Table 4 demonstrated a decrease in the minimum torque (M_L) of the kaolinite/SMR composites with K-CuX when compared to the standard CB/SMR and K-AX composites. A higher value of M_L in the K-A3/SMR composite corresponds to increased viscosity and is indicative of a greater extent of polymer-filler interaction in silanized kaolinite [38]. Nonetheless, the maximum torque (M_H), which correlates with stiffness, exhibited a slight decrease across all kaolinite/SMR composites. The K-A3/SMR composite demonstrated comprehensive performance on par with the standard. A high M_H indicates the development of a robust filler network. The incorporation of silanized kaolinite in the composites led to an increase in the M_H value, attributed to the formation of a higher number of crosslinks within the silicate moieties and thus improved interaction between the filler and the rubber matrix [39].

Payne effect of kaolinite/SMR composites

To characterize the degree of filler-filler and filler-polymer interactions, the measurement of the Payne effect [40] was conducted. The impact of the stiffening effect of fillers based on modified kaolinite was investigated. As the difference between the elastic component of the shear modulus *G′* at the minimum (0.28%) and the maximum deformation amplitude (100.02%): Δ*G′*= *G′*(0.28%) - *G′*(100.02%), the magnitude of the Payne effect, Δ*G′*, was determined [41]. Results obtained for G′ as a function of strain are depicted in Fig. 6a. With increasing amplitude, a reduction in the shear modulus *G′* is observed. The reduction in the modulus concerning the deformation is attributed to the gradual disintegration of the network formed by the filler particles, i.e., the interactions between the aggregates of the filler (breakdown of agglomerates) and between the filler particles and the rubber matrix dissipate. The decrease in *G′* with increasing deformation amplitude (Payne effect) is most pronounced in the standard CB/SMR composite because carbon black is characterized by smaller particles and a larger specific surface area compared to kaolinite, thereby anticipating the highest number of emergent interactions [42]. From the values of Δ*G′* in Fig. 6b, it can be inferred that this parameter is contingent on the characteristics of the applied fillers. In the standard composite containing carbon black, the filler network is optimally developed. Conversely, when employing 10 dsk of both modified and natural kaolinite, the values of *G′* and Δ*G′* diminished following vulcanization at lower amplitudes, indicating an enhanced dispersion of the kaolinite filler within the matrix and improved filler-rubber interactions. The lamellar kaolinite possesses a larger surface area, which enhances the interface between the rubber and kaolinite, thereby facilitating the formation of additional filler-rubber network structures. Marginally increased values of Δ*G′* and *G′* were noted for the silanized kaolinite K-A3.

T a b l e 5. Mechanical properties of kaolinite/SMR composites

Composite	Tensile strength at break MPa	Elongation at break %	Hardness Shore A IRHD
Ka/SMR	25.7 ± 0.9	429 ± 20	58 ± 1.6
K-Cu1/SMR	25.8 ± 0.9	405 ± 19	58 ± 3.8
K-Cu3/SMR	25.8 ± 0.4	455 ± 19	59 ± 0.7
K-A1/SMR	26.1 ± 0.3	455 ±12	62 ± 0.4
K-A3/SMR	25.6 ± 0.8	459 ± 14	62 ± 0.4
CB/SMR	27.5 ± 0.8	440 ± 9	65 ± 1.5

Mechanical properties of kaolinite/SMR composites

The results presented in Table 5 indicate a 2% and 2.9% increase in tensile strength at break of kaolinite/

SMR composites filled with K-A1 and K-A3, respectively. Regarding the type of modification agent, the incorporation of K-A1 or K-A3 resulted in higher T_{Sb} values compared to the standard CB/SMR, K-CuX/SMR, and Ka/SMR. As a direct indication of the reinforcing effect of the silanized kaolinite filler, the observed increase in tensile strength can be considered.

The capacity of the rubber composites to recover following mechanical loading was assessed via elongation at break. These findings corroborate the enhancement of the elasticity of composites with the incorporation of all kaolinite variants, providing definitive evidence of the enhanced interactions between the polymer and filler [43]. The maximum value of E_b was observed upon the addition of natural Ka. Hardness is the most readily observable property affected and relates to the increased cross-link density [44]. The hardness of composites comprising silanized kaolinite surpasses those with natural Ka and CuAc modified kaolinite.

The modification of kaolinite with silane through microwave heating has enhanced the reinforcing properties of kaolinite/SMR composites, even at a low concentration of 10 phr. The effective interactions between the silane-kaolinite and the rubber matrix are attributed to the increased hydrophobicity of the modified kaolinite [45, 46]. Organically modified kaolinite particles interact with rubber molecules by forming chemical bonds, facilitating physical adsorption, or achieving fine dispersion of kaolinite particles within the rubber, thereby restricting the movement of the rubber chains [47, 48].

CONCLUSIONS

The effect of copper acetate and silane modification on natural kaolinite treated with microwave heat was evaluated. The application of microwave radiation and its duration had a significant effect on shortening the kaolinite modification time from several days to minutes. FT-IR, EDX, SEM and thermal analyses showed that the properties of kaolinite were already changed after 30 min of chemical treatment/MW. Partial replacement of carbon black with silanized kaolinite resulted in a decrease in the vulcanization rate and acceleration of the curing process, thus improving the processing properties of the composites. Moreover, the production efficiency was increased and the energy consumption was significantly reduced. The composites containing silane-modified kaolinite showed good properties such as increased maximum torque, tensile strength and hardness, indicating some strengthening effect of the modified kaolinite. In practical applications, kaolinite is usually used in rubber compounds for conveyor belts or technical rubber. Modified kaolinite may prove useful in rubber compounds requiring high resistance to oxidation, acids and alkalis, coating tightness and as a barrier preventing air and moisture from entering the coating skeleton, as well as the required mechanical properties.

ACKNOWLEDGEMENTS

The authors would like to thank the Slovak Grant Agency KEGA for financial support (KEGA 008TnUAD-4/2025). The work was supported by the project Advancement and support of R&D for "Centre of Diagnostics and Quality Testing of Materials" in the Domains of the RIS3 SK", ITMS2014+:313011W442.

Authors contribution

A.F. – writing-original draft, investigation, methodology; J.S. – supervision, visualization, A.F,. J.P. – visualization, validation, A.D., M.P. – methodology, investigation, I.P., D.O. – visualization, validation, S.D., T.K. – investigation, methodology; M.D. – visualization, validation.

Funding

The work was funded by Slovak Grant Agency KEGA (KEGA 008TNUAD-4/2025). In addition, the work was supported by the project Advancement and support of R&D for Centre of Diagnostics and Quality Testing of Materials in the Domains of the RIS3 SK", ITMS2014+:313011W442.

Conflict of interest

The authors declare no conflict of interest.

REFERENCES

[1] Mañosa J., Gomez-Carrera A.M., Svobodova-Sedlackova A. *et al*.: *Applied Clay Science* **2022**, *228*, 106648. https://doi.org/10.1016/j.clay.2022.106648

[2] Neji A.B, Jridi M., Kchaou H. *et al*.: *Polymer Testing* **2020**, *84*, 106380. https://doi.org/10.1016/j.polymertesting.2020.106380

[3] Murray, H.H.: "Chapter 5 - Kaolin applications" in "Developments in Clay Science" (edit.: Anjum H., Ahmad S.W., Sharif R., Tausif M), Elsevier, Amsterdam 2006, p. 85. https://doi.org/10.1016/S1572-4352(06)02005-8

[4] Liang S., Li C., Dai L. *et al*.: *Applied Clay Science* **2018**, *161*, 282. https://doi.org/10.1016/j.clay.2018.04.038

[5] Pajtášová M., Pecušová B., Ondrušová D. *et al*.: *Polimery* **2024**, *69(4)*, 254. https://doi.org/10.14314/polimery.2024.4.6

[6] Kalendova A., Kupkova J., Urbaskova M. *et al*.: *Minerals* **2024**, *14(1)*, 93.

https://doi.org/10.3390/min14010093
[7] Sharma V., Agarwal S., Mathur A. *et al.*: *Journal of Industrial and Engineering Chemistry* **2024**, *133*, 38. https://doi.org/10.1016/j.jiec.2023.12.010
[8] Kloprogge J.T.: "Spectroscopic methods in the study of kaolin minerals and their modifications", Springer, Cham 2019, p. 428.
[9] Feriancová A., Pajtášová M., Pecušová B. *et al.*: *Applied Clay Science* **2019**, *183*, 105313. https://doi.org/10.1016/j.clay.2019.105313
[10] Makó É., Sarkadi Z., Ható Z. *et al.*: *Applied Clay Science* **2023**, *231*, 106753. https://doi.org/10.1016/j.clay.2022.106753
[11] Zhang S., Liu Q.F., Cheng H.F. *et al.*: *Applied Clay Science* **2018**, *151*, 46. https://doi.org/10.1016/j.clay.2017.10.022
[12] Valášková M., Rieder M., Matějka V. *et al.*: *Applied Clay Science* **2007**, *35(1–2)*, 108. https://doi.org/10.1016/j.clay.2006.07.001
[13] Frost R.L., Kristof J., Rintoul L. *et al.*: *Spectrochimica Acta A: Molecular and Biomolecular Spectroscopy* **2000**, *56(9)*, 1681. https://doi.org/10.1016/S1386-1425(00)00223-7
[14] Frost R.L., Kristof J., Paroz N. *et al.*: *Journal of Colloid and Interface Science* **1998**, *208(1)*, 216. https://doi.org/10.1006/jcis.1998.5780
[15] Roshin P., Sreelekshmi R.V., Menon A.R.R.: *Journal of Polymers and the Environment* **2018**, *26*, 39. https://doi.org/10.1007/s10924-016-0915-z
[16] Sidheswaran P., Bhat A.N., Ganguli P.: *Clays and Clay Minerals* **1990**, *38(1)*, 29. https://doi.org/10.1346/CCMN.1990.0380104
[17] Yang Y., Zhang H., Zhang K. *et al.*: *Applied Clay Science* **2020**, 185, 105366. https://doi.org/10.1016/j.clay.2019.105366
[18] Elimbi A., Tchakoute H.K., Njopwouo D.: *Construction and Building Materials* **2011**, *25(6)*, 2805. https://doi.org/10.1016/j.conbuildmat.2010.12.055
[19] Novikova L., Ayrault P., Fontaine C. *et al.*: *Ultrasonics Sonochemistry* **2016**, *31*, 598. https://doi.org/10.1016/j.ultsonch.2016.02.014
[20] Bakain R.Z., Al-Degs Y.S., Issa A.A. *et al.*: *Clay Minerals* **2014**, *49(5)*, 667. https://doi.org/10.1180/claymin.2014.049.5.04
[21] Mo S., Pan T., Wu F. *et al.*: *Journal of Environmental Management* **2019**, *238*, 257. https://doi.org/10.1016/j.jenvman.2019.03.003
[22] Li Z.J., Zhang X.R., Xu Z.: *Materials Technology* **2007**, *22(4)*, 205. https://doi.org/10.1179/175355507X236713
[23] Jóna E., Pajtášová M., Ondrušová D. *et al.*: *Journal of Analytical and Applied Pyrolysis* **2002**, *63(1), 17*. https://doi.org/10.1016/S0165-2370(01)00138-3
[24] Feriancová A., Dubec A., Pagáčová J. *et al.*: *Applied Clay Science* **2021**, *213*, 106259. https://doi.org/10.1016/j.clay.2021.106259
[25] Madejová J.: *Vibrational Spectroscopy* **2003**, *31(1)*, 1. https://doi.org/10.1016/S0924-2031(02)00065-6
[26] Mañosa J., Calvo-de la Rosa J., Silvello A. *et al.*: *Applied Clay Science* **2023**, *238*, 106918. https://doi.org/10.1016/j.clay.2023.106918
[27] Madejová J., Komadel P.: *Clays and Clay Minerals* **2001**, *49(5)*, 410. https://doi.org/10.1346/CCMN.2001.0490508
[28] Djomgoue P., Njopwouo D.: *Journal of Surface Engineered Materials and Advanced Technology* **2013**, *3(4), 275*. https://doi.org/10.4236/jsemat.2013.34037
[29] Ravindranathan P., Malla P.B., Komarneni S. *et al.*: *Catalysis Letters* **1990**, *6*, 401. https://doi.org/10.1007/BF00764008
[30] Berestova T.V., Kuzina L.G., Amineva N.A. *et al.*: *Journal of Molecular Structure* **2017**, *1137*, 260. https://doi.org/10.1016/j.molstruc.2017.02.023
[31] Pereira D.C., Faria D.L., Constantino R.L.: *Journal of the Brazilian Chemical Society* **2006**, *17(8)*, 1651. https://doi.org/10.1590/S0103-50532006000800024
[32] Alonso R.P., Rubio F., Rubio J. *et al.*: *Journal of Material Science* **2007**, *42*, *595*. https://doi.org/10.1007/s10853-006-1138-9
[33] Bois L., Bonhommé A., Ribes A. *et al.*: *Colloids and Surfaces A: Physicochemical and Engineering Aspects* **2003**, *221(1-3)*, 221. https://doi.org/10.1016/S0927-7757(03)00138-9
[34] Horváth E., Frost R.L., Makó É. *et al.*: *Thermochimica Acta* **2003**, *404(1–2)*, 227. https://doi.org/10.1016/S0040-6031(03)00184-9
[35] Mansa R., Ngassa Piegang B.G., Detellier C.: *Clays and Clay Minerals* **2017**, *65(3)*, 193. https://doi.org/10.1346/CCMN.2017.064059
[36] Ducháček V., Kuta A., Přibyl P.: *Applied Polymer Science* **1993**, *47(4)*, 743. https://doi.org/10.1002/app.1993.070470418
[37] Leblanc J.L.: *Applied Polymer Science* **2000**, *78(8)*, 1541. https://doi.org/10.1002/1097-4628(20001121)78:8<1541:AID-APP110>3.0.CO;2-1
[38] Zhang Y., Liu Q., Zhang S. *et al.*: *Applied Clay Science* **2016**, *124–125, 167*. https://doi.org/10.1016/j.clay.2016.02.002
[39] Payne A.R.: *Journal of Applied Polymer Science* **1962**, *6(19), 57*. https://doi.org/10.1002/app.1962.070061906
[40] Sattayanurak S., Sahakaro K., Kaewsakul W. *et al.*: *Polymer Testing* **2020**, *81*, 106173. https://doi.org/10.1016/j.polymertesting.2019.106173
[41] Xiao Y., Li B., Huang Y. *et al.*: *Applied Clay Science* **2024**, *261*, 107574. https://doi.org/10.1016/j.clay.2024.107574
[42] Raji V.V., Ramakrishnan S., Sukumar R. *et al.*: *Polymer International* **2015**, *64(11)*, 1585. https://doi.org/10.1002/pi.4956
[43] Liu Q., Zhang Y., Xu H.: *Applied Clay Science* **2008**, *42(1-2)*, 232. https://doi.org/10.1016/j.clay.2007.12.005

[44] Sreelekshmi R.V., Sudha J.D., Menon A.R.R.: *Polymer Bulletin* **2017**, *74*, 783. https://doi.org/10.1007/s00289-016-1745-9
[45] Ogbebor O.J., Okieimen F.E., Ogbeifun D.E. et al.: *Chemical Industry and Chemical Engineering Quarterly* **2015**, *21(4)*, 477. https://doi.org/10.2298/CICEQ140221003O
[46] Nasruddin, Augustini S., Sholeh M.: *IOP Conference Series: Materials Science and Engineering* **2020**, *1143*, 012010. https://doi.org/10.1088/1757-899X/1143/1/012010
[47] Zhang Y., Liu Q., Xiang J. *et al*.: *Polymer Science Series A* **2015**, *57*, 350. https://doi.org/10.1134/S0965545X15030177

Received 24 I 2025.
Accepted 12 II 2025.